Evaluation of AMSR-E retrievals and GLDAS simulations against observations of a soil moisture network on the central Tibetan Plateau

Yingying Chen,[1] Kun Yang,[1] Jun Qin,[1] Long Zhao,[1,2] Wenjun Tang,[1] and Menglei Han[1,2]

Received 10 December 2012; revised 25 January 2013; accepted 25 February 2013.

[1] A multi-scale soil moisture and temperature monitoring network, consisting of 55 soil moisture and temperature measurement stations, has been established in central Tibetan Plateau (TP). In this study, the station-averaged surface soil moisture data from the network are used to evaluate four soil moisture products retrieved from the Advanced Microwave Scanning Radiometer-Earth Observing System (AMSR-E) and four land surface modeling products from the Global Land Data Assimilation System (GLDAS). Major findings are (1) none of the four AMSR-E products provides reliable estimates in the unfrozen season, in terms of the mission requirement of the root mean square error (RMSE) $< 0.06\ m^3m^{-3}$. These algorithms either evidently overestimate soil moisture or obviously underestimate it, although some of them showed the soil moisture dynamic range, indicating that the retrieval algorithms have much space to be improved for the cold semi-arid regions. (2) The four GLDAS models tend to systematically underestimate the surface soil moisture (0–5 cm) while well simulate the soil moisture for 20–40 cm layer. In comparison with the satellite surface soil moisture products, three among the four models give low *RMSE* and *BIAS* values, but still falling out of the acceptable range. The causes for the modeling biases in this cold region were discussed.

Citation: Chen, Y., K. Yang, J. Qin, L. Zhao, W. Tang and M. Han (2013), Evaluation of AMSR-E retrievals and GLDAS simulations against observations of a soil moisture network on the central Tibetan Plateau, *J. Geophys. Res. Atmos.*, *118*, doi:10.1002/jgrd.50301.

1. Introduction

[2] Soil moisture controls a variety of the hydro-meteorological, hydro-climatological, ecological, and bio-geochemical processes in various spatial and temporal scales [e.g., *Milly and Dunne*, 1994; *Douville and Chauvin*, 2000; *Koster et al.*, 2004; *Balsamo et al.*, 2009; *Falloon et al.*, 2011], but conventional observations are too sparse to satisfy the needs for improving remote sensing and land surface modeling [e.g., *Crow et al.*, 2012], which have potential to provide regional soil moisture datasets that are urgently required for many research and application purposes.

[3] Early field and aircraft experiments demonstrated that the low-frequency microwave emissions (passive and active) are related to the surface soil moisture [e.g., *Schmugge*, 1977], thus the soil moisture can be potentially retrieved from the microwave signals. Over the past two decades, great efforts have been made within the international remote sensing community to develop soil moisture products from both active and passive microwave signals [e.g., *Jackson*, 1993; *Njoku et al.*, 2006; *Wagner et al.*, 2003; *Koike et al.*, 2004; *Owe et al.*, 2008; *Kerr et al.*, 2012; *Scipal et al.*, 2009; *Entekhabi et al.*, 2010] with the launch of several microwave sensors. The accuracy of soil moisture estimated from satellite sensors needs to be characterized before being used in practical applications. Some studies have assessed satellite soil moisture products through inter-comparisons with scale-comparable model simulations [e.g., *Wagner et al.*, 2003; *Rüdiger et al.*, 2009], other satellite soil moisture product [*de Jeu et al.*, 2008], or both of them [e.g., *Scipal et al.*, 2008; *Dorigo et al.*, 2010], but evaluations against directly measured "ground truth" are needed. It is risky to use measurements at a single station to represent the ground truth because of the high spatial variability of soil moisture; and therefore, dense soil moisture networks are required for valid evaluations [e.g., *Yang et al.*, 2009a]. With the development of the International Soil Moisture Network [e.g., *Dorigo et al.*, 2011], many evaluation activities were conducted in North America [e.g., *Jackson et al.*, 2010, 2012; *Bitar et al.*, 2012; *Collow et al.*, 2012; *Gherboudj et al.*, 2012], Europe [e.g., *Brocca et al.*, 2011; *Albergel et al.*, 2012, *Dall'Amico et al.*, 2012; *Sánchez et al.*, 2012; *Lacava et al.*, 2012], and Australia [e.g., *Draper, et al.*, 2009; *Merlin et al.*, 2012], but less evaluation activities were performed in Asia [*Su et al.*, 2011] and Africa [*Gruhier et al.*, 2010]. In particular, most of these studies are conducted in temperate climate

[1]Key Laboratory of Tibetan Environment Changes and Land Surface Processes, Institute of Tibetan Plateau Research, Chinese Academy of Sciences, Beijing, China.
[2]University of Chinese Academy of Sciences, Beijing, China.

Corresponding author: Yingying Chen, Institute of Tibetan Plateau Research, CAS, Building 3, Courtyard 16, Lin Cui Road, Chaoyang District, Beijing 100101, China. (chenyy@itpcas.ac.cn)

2169-8996/13/jgrd.50301

regions; and therefore, more evaluations in other climate regions are anticipated to test the applicability of a remote sensing algorithm.

[4] Meanwhile, land surface models (LSMs) have the potential to estimate regional soil moisture distribution, but their accuracy is hindered by model deficiencies, and uncertainties in both model parameters and atmospheric forcing. Soil moisture simulated by LSMs was also evaluated against point-scale measurements [e.g., *Boisserie et al*., 2006; *Li et al*., 2007; *Albergel et al*., 2012]. However, evaluation of a model's performance is a difficult task due to the scale mismatching issue [*Prigent et al*., 2005].

[5] In this study, we evaluated four satellite products and four land surface modeling outputs of soil moisture in the central Tibetan Plateau (TP), where the weather is cold and soil moisture has large seasonal variations. In a recent study, *Su et al*. [2011] have evaluated satellite soil moisture products in a dry area of the western TP and a semi-humid area of the eastern TP against observations from two soil moisture networks. The products were also evaluated for the central TP, but the number of measuring stations is limited and the stations are deployed within a small area. In this study, we evaluated soil moisture products using a much denser multi-scale network that has been constructed recently. In the following parts, the observation network and the soil moisture products will be briefly introduced in section 2; the results and discussions will be presented in section 3 and section 4, separately; finally, the concluding remarks are given in section 5.

2. Data and Methods

2.1. Ground Data

[6] Tibetan Plateau (TP) is the highest plateau in the world with an average elevation of over 4000 m above sea level (ASL) and an area of approximately 2.5×10^6 km^2, which has been experiencing significant hydro-climatic change in the past decades [e.g., *Yang et al*., 2011; *Qin et al*., 2009]. A multi-scale soil moisture and temperature monitoring network is deployed in the central TP around Naqu city (hereafter called Naqu network, see Figure 1) with an average elevation of 4650 m ASL. The terrain is fairly flat with rolling hummocks and hills. Due to low air mass and clear sky, the land surface receives much stronger solar radiation than low elevation regions [*Yang et al*., 2010]; thus, the weather experiences large diurnal variations and evident seasonal changes. The strong land-atmosphere interactions in summer induce very active local convection in this high elevation area. The annual precipitation is ~500 mm, and 75% of this amount is received from May to October, due to the significant impact of the South Asian summer monsoon. Because of the cold environment, soil thawing and freezing occur around May and November, respectively. The area is mostly covered by alpine grassland, consisting of tiles of prairie grasses and meadows, with moderately low aboveground biomass [the normalized difference vegetation index (NDVI) ~0.15–0.51, derived from 2000–2006 Moderate Resolution Imaging Spectroradiometer data], thus the vegetation exerts less impacts on soil moisture retrieval. Therefore, this low-biomass and large soil moisture range make Naqu network be an ideal site for evaluations of satellite soil moisture products.

[7] The buildup of Naqu network started in 2010. The first 30 Soil Moisture and Temperature Measurement System (SMTMS) stations (see black rectangles in Figure 1) were deployed since July 2010 within a $1° \times 1°$area (hereafter called the large coarse network) to approximately match a Global Climate Model (GCM) grid. Then, 20 SMTMS stations (see white triangles in Figure 1) were added in July 2011 to enhance a $0.25° \times 0.25°$observing network (31.5–31.75°N, 91.75–92.0°E, hereafter called the small dense network). The network was further enhanced by adding five stations in the summer, 2012. The sensors used in the network are EC-TM and 5TM capacitance probes manufactured by Decagon Devices (http://www.decagon.com/). The sensor can simultaneously measure soil moisture and temperature with an accuracy of ± 0.03 m^3 m^{-3}/± 1°C and resolution of 0.001 m^3 m^{-3}/0.1°C for mineral soils. Note

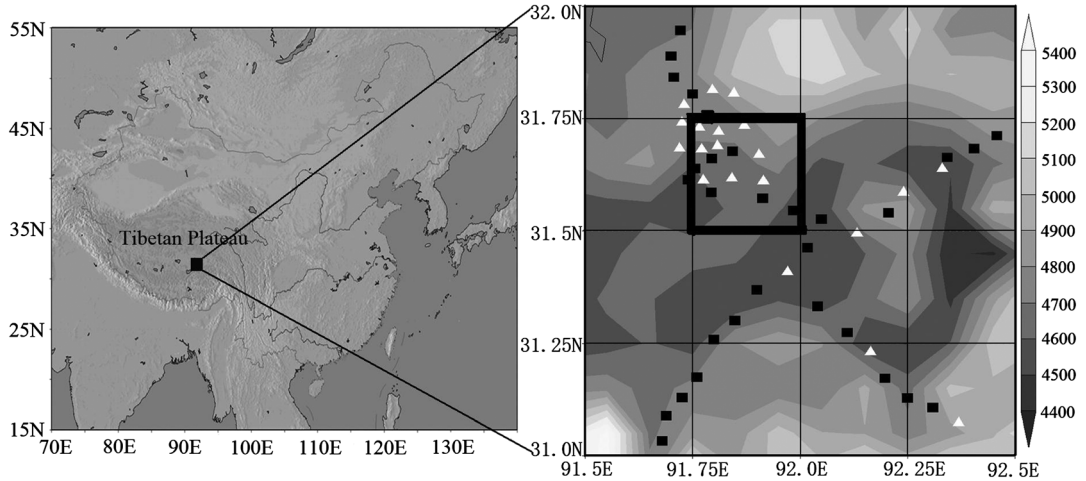

Figure 1. The location of the soil moisture network within a $1° \times 1°$area (the large coarse network) around Naqu of the central TP. The bold black square in the right panel denotes a $0.25° \times 0.25°$observing network (the small dense network) with enhanced observations. Black rectangles denote 30 stations deployed in 2010, and white triangles denote 20 stations deployed in 2011.

that only the liquid water content is measured within frozen soils during winter. At each station, one sensor is obliquely inserted into 0–5 cm topsoils, and other three are horizontally inserted at 10 cm, 20 cm, and 40 cm depths, respectively. Measuring time interval is set to 30 min, and each record reflects the average state of soil moisture over the past half-hour. Meanwhile, soil texture and soil organic carbon (SOC) content were measured for each 5 cm soil layer at each station. Within the topsoil of the alpine grasslands, high SOC contents are found due to high accumulative rate under the cold conditions. This may significantly affect the soil thermal/hydraulic properties [*Chen et al*., 2012] and soil dielectricity, and thus the effect of SOC has been taken into account for the sensor calibration.

[8] A two-step sensor calibration approach is developed to make the observational data reliable. First, the official relationship to convert the apparent dielectric permittivity into soil water content, which is developed for mineral soil, is replaced by the equation developed by *Schaap et al*. [1996] that considers the effects of soil organic matter, a major soil component in this region. Second, the derived soil water content in the first step is linearly calibrated with measured soil moisture by the gravimetric method in laboratory. Note that the sensor can only measure liquid water content and thus the measurements cannot denote the total water in frozen soil. With this in mind, the conclusions are mainly derived from the evaluation during unfrozen season in this study.

2.2. Soil Moisture Products

2.2.1. Satellite Data

[9] The Advanced Microwave Scanning Radiometer-Earth Observing System (AMSR-E) is a radiometer operating onboard the Aqua satellite of the National Aeronautics and Space Administration (NASA) since May 2002. AMSR-E sensor has provided passive microwave measurements at six bands, ranging from 6.9 to 89 GHz at HH-VV polarization, with daily ascending (13:30 equatorial local crossing time) and descending (01:30 equatorial local crossing time) overpasses. It provides the opportunity to retrieve the first standard satellite soil moisture product with an expectant accuracy goal [i.e., the root mean square error (RMSE) $<0.06\,m^3\,m^{-3}$] [*Njoku et al*., 2003]. Several soil moisture products have been developed based on AMSR-E data [e.g., *Njoku and Chan*, 2006; *Jackson*, 1993; *Koike et al*., 2004; *Paloscia et al*., 2006; *Owe et al*., 2008], and a few evaluation efforts of these products have been performed against observations from dedicated soil moisture evaluation site [e.g., *Jackson et al*., 2010; *Brocca et al*., 2011; *Draper*, *et al*., 2009; *Su et al*., 2011; *Gruhier et al*., 2010]. These evaluations show diverse performance for AMSR-E products in different regions; the most encouraging results are found for the semi-arid regions with light vegetation.

[10] In this study, the four interested AMSR-E products are: the NASA standard soil moisture product [*Njoku and Chan*, 2006], the Japan Aerospace Exploration Agency (JAXA) soil moisture product [*Koike et al*., 2004; *Lu et al*., 2009; *Fujii et al*., 2009], and both the C-band and X-band soil moisture products developed using the Land Parameter Retrieval Model (hereafter called LPRM_C and LPRM_X products) [*Owe et al*., 2008]. The daily level-3 data of these soil moisture products are evaluated in this study. It should be noted that the NASA and JAXA standard products were retrieved using X-band signal to avoid the well-known radio-frequency interference with C-band observations in some regions, but the LPRM product used both C-band and X-band signals. In addition, the time period for the NASA and LPRM data is from 1 August 2010 to 20 September 2011; while the time period for JAXA data is from 1 August 2010 to 31 July 2011.

2.2.2. Model Data

[11] The Global Land Data Assimilation System (GLDAS) is developed to generate optimal fields of land surface states and fluxes by integrating satellite- and ground-based observational data products, using land surface modeling and data assimilation techniques [*Rodell et al*., 2004]. GLDAS drives multiple, offline LSMs, integrates a huge quantity of observation based data and executes globally at multi-resolutions. A vegetation-based "tiling" approach is used to simulate sub-grid scale variability, with a 1-km global vegetation dataset as its basis. Soil and elevation parameters are derived from high resolution global datasets. Observation-based precipitation and downward radiation products and the best available analyses from atmospheric data assimilation systems are employed to force the models. GLDAS data are archived and distributed at the website of the Goddard Earth Sciences Data and Information Services Center (http://disc.sci.gsfc.nasa.gov/hydrology/data-holdings).

[12] In this study, the 3-hourly 0.25° and 1.0° GLDAS Version 1 products (GLDAS-1) are used. The GLDAS-1 products integrate outputs from four LSMs: Community Land Model (CLM), Noah model, MOSAIC model, and Variable Infiltration Capacity (VIC) Model. At present, only Noah provides both 0.25° and 1° products, while other three LSMs provide only 1° products.

2.3. Methods

[13] First, we evaluate AMSR-E surface soil moisture products. Considering the spatial representativeness issue, we averaged the measurements at 30 stations (black rectangles in Figure 1) to represent the values for the large coarse network. The station-averaged surface soil moisture (0–5 cm) is compared with AMSR-E data averaged over all grids within the large coarse network. The ascending and the descending passes are evaluated, separately, as their retrieval accuracy may be different. Their performance is given by the mean bias (*BIAS*), the root mean square error (*RMSE*), and the determination coefficient (R^2). We also evaluate the accuracy of AMSR-E soil moisture at the small dense network with enhanced measurements. Within this grid and its neighbor, eight stations started measurements in 2010, and the other nine stations started in 2011. To give a longer-term evaluation, we used the average over the eight stations for the evaluation. In addition, a discussion on sensitivity to the measurement density will be given in section 4.1.

[14] Then, we evaluate GLDAS simulated soil moisture outputs against the station-averaged soil moisture observations for 0–5 cm and for 10–40 cm (the average of values at 10, 20, and 40 cm), respectively, for the large coarse network. Also, the soil moisture measurements for the small dense network are used to evaluate the output from Noah, which is the only one among the four models that has a spatial resolution comparable to the small dense network.

3. Results

3.1. AMSR-E Soil Moisture Products

[15] The station-averaged soil moisture exhibits an obvious seasonal variation, ranging from 0.05 to 0.42 $m^3 m^{-3}$ (Figure 2), in the large coarse network. The surface soil (0–5 cm) is frozen at the beginning of November with the soil moisture dropping abruptly from above 0.2 to below 0.1 $m^3 m^{-3}$ and is thawed at the beginning of May with abruptly soil moisture rising. Figures 2 and 3 present the time series and the scatter plot of the station-averaged soil moisture and four AMSR-E estimates for both the descending and the ascending orbits for the period from 1 August 2010 to 20 September 2011. The error metrics are presented in Table 1 for the unfrozen season (May to October) and the frozen season (November to April), respectively.

[16] For the descending orbit, Figures 2a and 3a indicate that the NASA product evidently underestimates soil moisture in the unfrozen season while slightly overestimates soil moisture in the frozen season and exhibits a dampened range compared to the observed one. This seems to be a common phenomenon found by many other studies [e.g., *Jackson et al.*, 2010]. The NASA product gives the largest *BIAS* and *RMSE* as well as the minimum R^2 for the unfrozen season (Table 1). Figure 2a also suggests that both JAXA and LPRM products can reflect the soil moisture dynamic range but with larger amplitude than observations. The JAXA product slightly underestimates the soil moisture in average

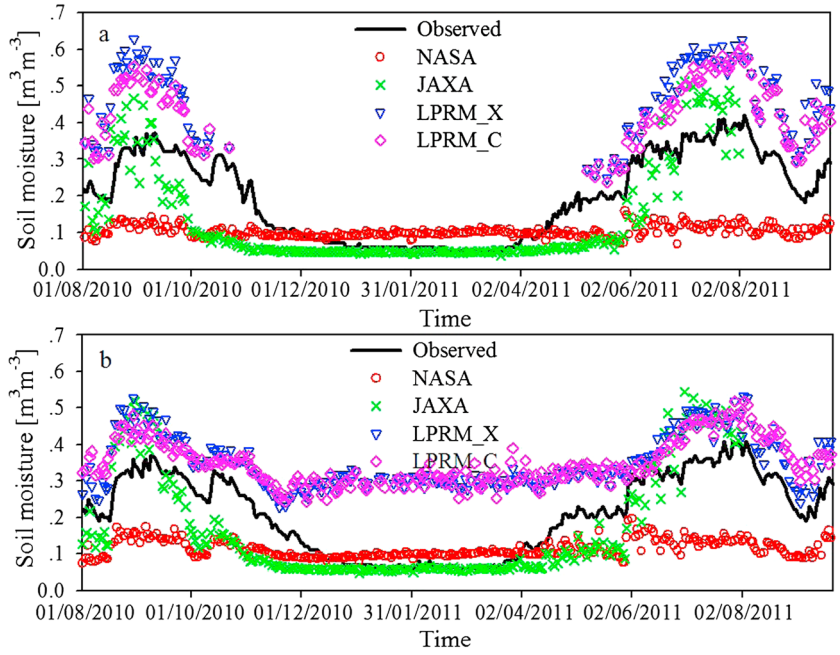

Figure 2. The time series of the station-averaged soil moisture and the four AMSR-E estimated ones for (a) the descending orbit and (b) the ascending orbit, separately, from 1 August 2010 to 20 September 2011 for the large coarse network. Note: both LPRM_C and LPRM_X products are presented; the time period for the JAXA data is from 1 August 2010 to 31 July 2011.

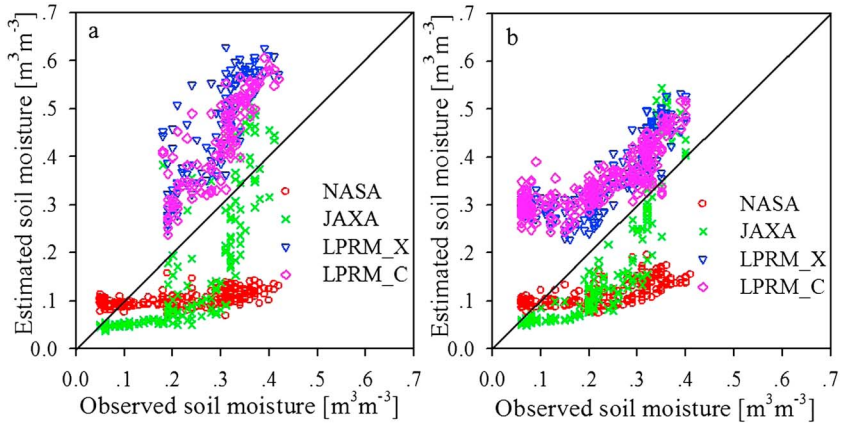

Figure 3. The scatter plots of the station-averaged soil moisture and the four AMSR-E estimated ones for (a) the descending orbit and (b) the ascending orbit, respectively, for the large coarse network.

Table 1. Error metrics of AMSR-E estimated soil moisture for Naqu network[a]

Period	Area	Products	Descending				Ascending			
			BIAS	*RMSE*	R^2	*No.*	*BIAS*	*RMSE*	R^2	*No.*
Unfrozen season	Large coarse network	NASA	−0.18	0.19	0.315	161	−0.17	0.17	0.479	161
		JAXA	−0.06	0.12	0.547	115	−0.01	0.10	0.687	114
		LPRM_C	0.14	0.15	0.729	120	0.09	0.10	0.653	146
		LPRM_X	0.17	0.18	0.683	120	0.09	0.10	0.768	146
	Small dense network	NASA	−0.16	0.17	0.181	161	−0.15	0.16	0.381	162
		JAXA	0.07	0.17	0.439	101	0.08	0.17	0.591	113
		LPRM_C	0.10	0.12	0.671	145	0.05	0.06	0.703	161
		LPRM_X	0.13	0.15	0.670	145	0.06	0.07	0.759	161
Frozen season	Large coarse network	NASA	0.01	0.04	0.001	125	−0.01	0.05	0.187	125
		JAXA	−0.03	0.05	0.453	113	−0.04	0.06	0.578	114
		LPRM_C	-	-	-	-	0.19	0.20	0.045	107
		LPRM_X	-	-	-	-	0.19	0.20	0.005	107
	Small dense network	NASA	0.02	0.05	0.001	126	0.00	0.05	0.180	133
		JAXA	−0.04	0.07	0.678	133	−0.02	0.05	0.468	114
		LPRM_C	-	-	-	-	0.15	0.15	0.297	125
		LPRM_X	-	-	-	-	0.15	0.15	0.166	125

[a]*BIAS* is the mean bias (unit: $m^3\,m^{-3}$), *RMSE* is the root mean square error (unit: $m^3\,m^{-3}$), R^2 is the determination coefficient, and *No.* is the sample number.

with the minimum *BIAS* and *RMSE* for the unfrozen season. The LPRM_C and LPRM_X products obviously overestimate the soil moisture but with high R^2 for the unfrozen season; meanwhile, the LPRM_C product performs better than the LPRM_X product (Figures 2a and 3a). Note that the descending LPRM data are not available in the frozen season. As shown in Table 1, none of the four soil moisture estimates can give an acceptable *RMSE* value (i.e., *RMSE* $<0.06\,m^3\,m^{-3}$).

[17] For the ascending orbit, the results for the four AMSR-E products are somewhat better than the results for the descending orbit for the unfrozen season. As indicated in Table 1, the products for the ascending orbit have small *BIAS* and *RMSE*. This conflicts with the expectation that a retrieval method may be reliable for nighttime overpass (i.e., the descending orbit), when the near-surface soil moisture and temperature profiles are more uniform than daytime overpass (i.e., the ascending orbit). *Brocca and Hasenauer*, 2011 also found that the retrieval from the daytime overpass seem to be more accurate and suggested that the daytime overpass have a positive effect at certain vegetation densities. Some studies found that there is no obvious difference between the daytime overpass and the nighttime overpass for AMSR-E soil moisture products [e.g., *Jackson et al*., 2010] and for Soil Moisture and Ocean Salinity soil moisture products [e.g., *Jackson et al*., 2012; *Sánchez et al*., 2012]. However, many other studies [e.g., *Draper et al*., 2009; *Gruhier et al*., 2010; *Su et al*., 2011] only evaluated the nighttime overpass AMSR-E soil moisture products with the abovementioned expectation. Note that the LPRM soil moisture data are available in the frozen season for the ascending orbit, but the large *BIAS* and *RMSE* indicate that the LPRM algorithm does not work well for the frozen season. Again, the *RMSE* for the four ascending AMSR-E products fall out of the acceptable range. Differing from other products, the LPRM products performs rather different between the ascending and the descending orbits (Table 1). Recent studies [*Jackson et al*., 2010; *Su et al*., 2011] suggest that the error in LPRM is most likely associated with the retrieval of the surface temperature.

[18] AMSR-E soil moisture products are also evaluated against station-averaged observations of the small dense network. The grid value is averaged over the six stations within the grid and two adjacent stations that are set up since 2010. Figure 4 shows the time series for the descending and the ascending orbits, respectively. The error metrics are also presented in Table 1. Similar to the results for the large coarse network, the NASA algorithm still exhibits a dampened range while the JAXA algorithm and the LPRM can reflect the seasonal variation of soil moisture. Also, the results for the ascending orbit are better than the results for the descending orbit in unfrozen season. For the LPRM algorithm, the soil moisture climatology is still obviously different for the ascending and the descending orbits; the ascending product performs much better than the descending product and almost meets the mission accuracy requirement in unfrozen season (Table 1). An exception is that the JAXA algorithm tends to reach its global maximum value ($0.6\,m^3\,m^{-3}$) under very wet conditions in the small grid, which lead to an overestimation of soil moisture. In a word, the evaluation results for the small dense network are consistent with the results for the large coarse network.

[19] The aforementioned results indicate that the four AMSR-E derived soil moisture products cannot meet the mission accuracy requirement (i.e., the *RMSE* $< 0.06\,m^3\,m^{-3}$) in unfrozen season. The NASA algorithm exhibits a dampened range while the JAXA algorithm and the LPRM can reflect the seasonal variation of soil moisture but with too large amplitude. The ascending orbit products perform somewhat better than the descending orbit products in the unfrozen season. The evaluation results for the small dense network are consistent with the results for the large coarse network.

3.2. GLDAS Simulated Soil Moisture

[20] In GLDAS, the soil layer specification is model-dependent, as shown in Table 2. The simulated soil moisture is the depth-averaged values. To better match the depths between the simulated soil moisture and the measured ones, the averaged values for the upmost two layers of CLM (0–4.5 cm), the values for the first layer of Noah (0–10 cm), MOSAIC (0–2 cm), and VIC (0–10 cm) are evaluated against the observed ones for 0–5 cm. The simulated soil moisture for the second layer of Noah (10–40 cm) and the averaged values for the fourth to sixth layer of CLM (9.1–49.3 cm) are also evaluated against the average of observations at

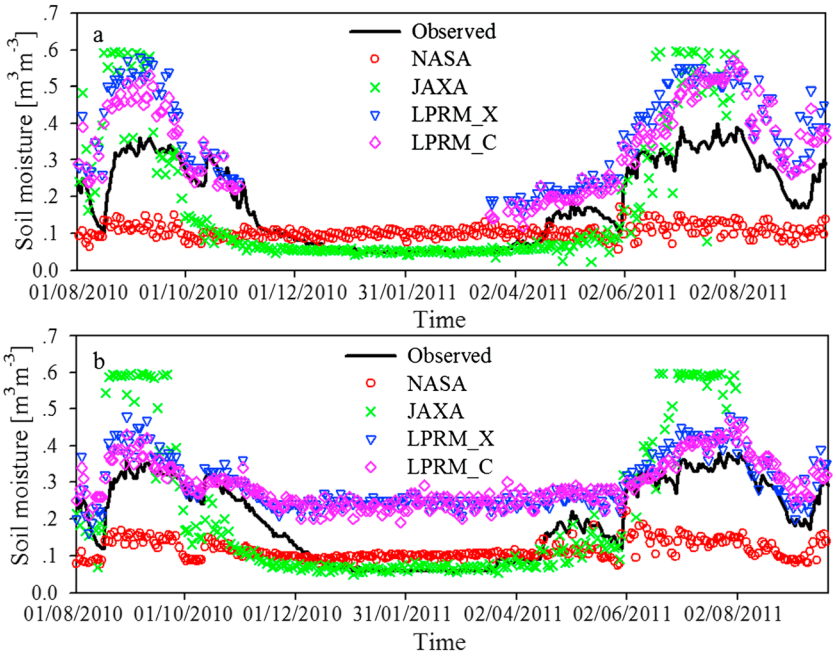

Figure 4. The time series of the station-averaged soil moisture and the four AMSR-E estimated ones for (a) the descending orbit and (b) the ascending orbit, separately, for the small dense network.

Table 2. The specified depths of soil layers for four LSMs in GLDAS

LSMs	Vertical Layers
CLM (10 layers)	0–1.8, 1.8–4.5, 4.5–9.1, 9.1–16.6, 16.6–28.9, 28.9–49.3, 49.3–82.9, 82.9–138.3, 138.3–229.6, and 229.6–343.3 cm
Noah (four layers)	0–10, 10–40, 40–100, and 100–200 cm
Mosaic (three layers)	0–2, 2–150, and 150–350 cm
VIC (three layers)	0–10, 10–160, and 160–190 cm

10, 20, and 40 cm. This evaluation is not conducted for VIC and MOSAIC, as the model depth does not match the observed one. In addition, all the simulated soil moisture for the frozen season (November 2010 to April 2011) are not evaluated, as the models provide the total soil moisture (both liquid and solid water) data while the sensor only measured liquid water.

[21] Figure 5 displays the time series of the simulated soil moisture and the station-averaged ones for 0–5 cm and 10–40 cm, respectively. Table 3 gives the error metrics. Figures 5a and 5b show that the four models can reflect the seasonal variation for surface soil moisture but systematically underestimate surface soil moisture, as indicated by the negative *BIAS* values in Table 3. Among these LSMs, VIC model gives the lowest *BIAS* ($-0.02\,m^3\,m^{-3}$) and *RMSE* ($0.05\,m^3\,m^{-3}$). However, VIC also gives the lowest R^2 (0.358). Noah model gives moderate *BIAS* ($-0.06\,m^3\,m^{-3}$) and *RMSE* ($0.08\,m^3\,m^{-3}$). The performance of CLM is slightly poorer than Noah. MOSAIC has the largest *RMSE*, perhaps due to the soil depth mismatch between the model (0–2 cm) and the observation (0–5 cm). Figure 5c and the error metrics in Table 3 indicate that Noah and CLM well simulate the soil moisture for 10–40 cm soil layer. In comparison with AMSR-E algorithms, the LSMs give low *RMSE* and *BIAS* values except for Mosaic. However, the errors are still large and the R^2 are low for GLDAS surface soil moisture outputs (Table 3).

[22] The station-averaged soil moisture for the small dense network is also used to evaluate the 0.25° Noah outputs. The error metrics are presented in Table 3, and the performance is similar to that for the large coarse network.

[23] In a word, the GLDAS LSMs systematically underestimate the moisture for the surface soil layer but well simulate the moisture below the surface soil layer for this region. This issue will be discussed in section 4.2.

4. Discussions

4.1. Sensitivity to the Measurement Density

[24] In the aforementioned evaluation for the small dense network, we used eight stations that have data records since 2010. The network was enhanced in 2011, with nine additional stations installed within the small dense network. Figure 6 shows the soil moisture time series averaged over the eight stations and the one averaged over all 17 stations for the period from 1 July 2011 to 20 September 2011. The latter is slightly larger than the former, with their mean difference of $0.021\,m^3\,m^{-3}$, root mean square difference of $0.024\,m^3\,m^{-3}$, and R^2 of 0.99. We re-evaluated AMSR-E soil moisture products against the all-station averaged values. The error metrics in Table 4 show *BIAS* and *RMSE* change slightly, but the errors are still too large to meet the mission requirement. Regarding the Noah simulation, its

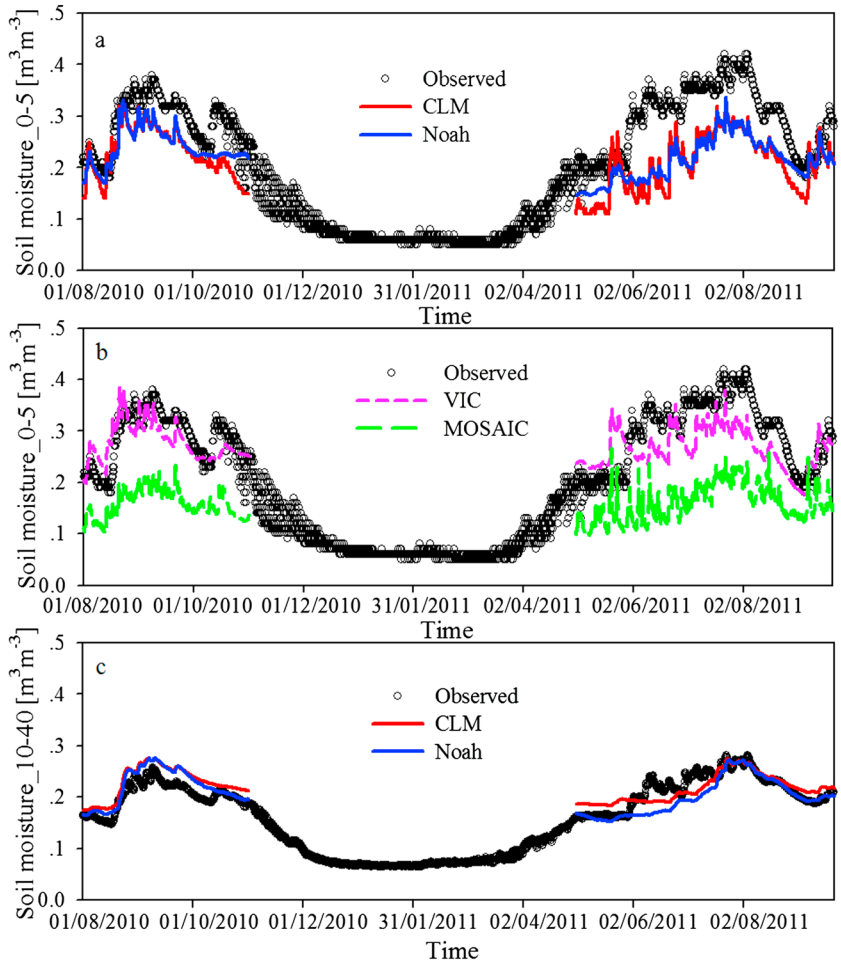

Figure 5. The time series of the station-averaged soil moisture and the simulated ones (a) for 0–5 cm by CLM and Noah, (b) for 0–5 cm by VIC and MOSAIC, and (c) for 10–40 cm by CLM and Noah for the large coarse network. Note: all the simulated soil moisture for the frozen season are not evaluated, as the models provide the total soil moisture (both liquid and solid water) data while the sensor only measured liquid water. The deeper layer data from MOSAIC and VIC are not evaluated because the depths in the models do not matchup with the depth of the observation.

Table 3. Error metrics of GLDAS simulated soil moisture (for 0–5 cm and 20–40 cm, respectively) during the unfrozen season for the Naqu network

Area	Depth	LSMs	*BIAS* ($m^3\ m^{-3}$)	*RMSE* ($m^3\ m^{-3}$)	R^2	*No.*
Large coarse network	0–5 cm	CLM	−0.08	0.09	0.473	1878
		Noah	−0.06	0.08	0.483	1878
		VIC	−0.02	0.05	0.358	1878
		Mosaic	−0.13	0.14	0.491	1878
	10–40 cm	CLM	0.01	0.02	0.609	1878
		Noah	0	0.02	0.585	1878
Small dense network	0–5 cm	Noah	−0.07	0.09	0.466	1878
	10–40 cm	Noah	−0.04	0.04	0.528	1878

performance becomes even worse when evaluated with the all-station averaged soil moisture.

4.2. Underestimation of Surface Soil Moisture in GLDAS

[25] It is well known that uncertainties in atmospheric forcing and model parameters cause simulation errors. In this study, the four GLDAS LSMs systematically underestimate the surface soil moisture, but two (CLM and Noah) among them can well simulate the 10–40 cm soil moisture in the central TP. In the following, we investigate the cause of this phenomenon.

[26] Concerning soil moisture simulation, precipitation and soil properties are two dominant factors. First, the measured precipitation at CMA (China Meteorological Administration) Naqu station, which is located at the center of our network, is compared with GLDAS precipitation. Figure 7 shows the

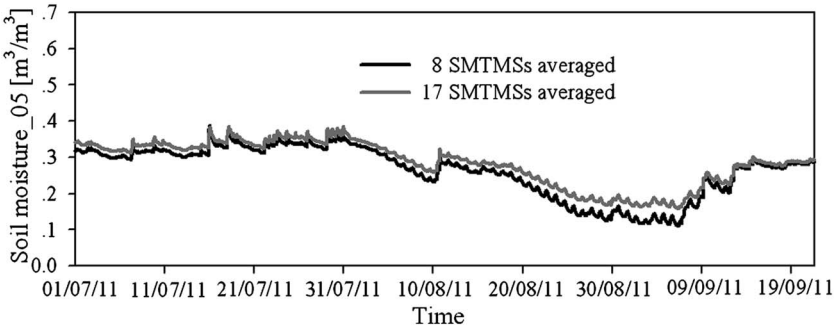

Figure 6. The time series of surface soil moisture averaged over the eight stations deployed in 2010 and over all 17 stations within the small dense network from 1 July 2011 to 20 September 2011.

Table 4. Error metrics of AMSR-E soil moisture against the averaged values over eight stations deployed in 2010 (outside the parentheses) and against the averaged values over all 17 stations (inside the parentheses) for the period of 1 July to 20 September 2011 for the small dense network[a]

	Products	*BIAS* ($m^3\ m^{-3}$)	*RMSE* ($m^3\ m^{-3}$)	R^2	*No.*
Descending	NASA	−0.15(−0.17)	0.17(0.18)	0.28(0.271)	57
	JAXA	0.19(0.17)	0.22(0.21)	0.379(0.221)	21
	LPRM_C	0.17(0.15)	0.18(0.15)	0.724(0.764)	52
	LPRM_X	0.19(0.16)	0.19(0.17)	0.696(0.719)	52
Ascending	NASA	−0.14(−0.16)	0.15(0.17)	0.628(0.626)	57
	JAXA	0.26(0.24)	0.26(0.24)	0.159(0.163)	21
	LPRM_C	0.1(0.08)	0.11(0.08)	0.696(0.75)	57
	LPRM_X	0.09(0.07)	0.1(0.08)	0.742(0.767)	57

[a]The period for the JAXA data is only from 1 July 2011 to 31 July 2011.

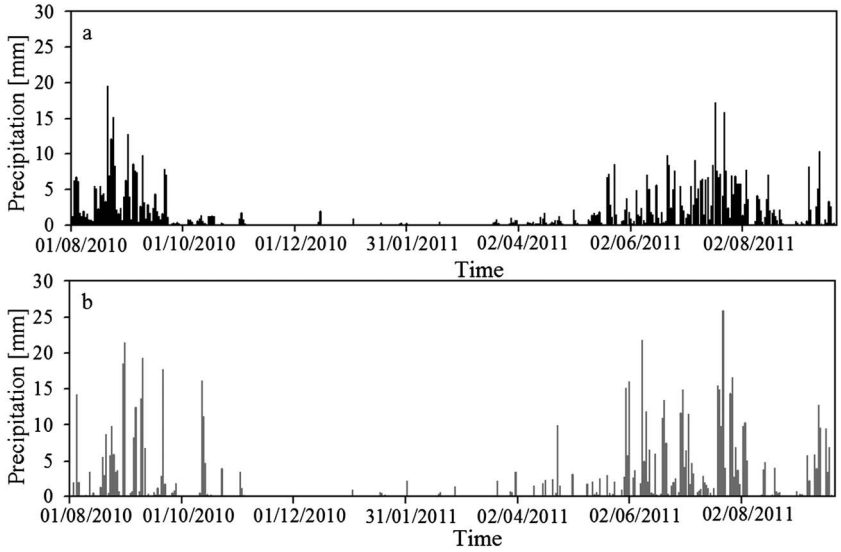

Figure 7. The time series of (a) the GLDAS daily precipitation and (b) the observed one for Naqu station from 1 August 2010 to 20 September 2011 for the large coarse network.

time series of GLDAS daily precipitation and the observed one at CMA Naqu station from 1 August 2010 to 20 September 2011. During this period (a total of 416 days), the total amount of GLDAS precipitation (659 mm) is slightly smaller than the observed one (720 mm), but the precipitation events in GLDAS (141 days with daily precipitation ≥ 1 mm) are more frequent than those measured at CMA Naqu station (106 days with daily precipitation ≥ 1 mm). As a result, LSMs may yield higher soil water content when being driven by GLDAS precipitation than being driven by the observed precipitation. Therefore, the precipitation is not the main cause leading to the LSM's underestimation of surface soil moisture.

[27] On the other hand, the areal soil hydraulic properties may significantly impact the simulation of the surface soil moisture. Several studies indicate that SOC substantially affect the soil thermal/hydraulic properties

[e.g., *Yang et al*., 2005; *Lawrence and Slater*, 2008; *Chen et al*., 2012]. According to our measurements in Naqu network, the SOC content is substantially high within the topsoil (mean volumetric content of 28.8% for 0–5 cm layer) while rapidly decreases with soil depth (around 6.2% at depth of 40 cm). This lead to evident soil stratification, for example, large soil porosity and water retention capability for the topsoil but low values for the deeper soil. Therefore, we observed high surface soil water content in this region. However, this SOC-induced stratification of soil properties is not well represented in GLDAS LSMs, which causes the significant underestimation of the surface soil moisture. More detailed investigations are needed to clarify this issue. In addition, the accuracy of the simulated evaporation may also affect the soil moisture in the model. Evaporation is determined by several transfer resistances (e.g., turbulent transfer resistance, canopy stomatal resistance, and soil evaporation resistance), and each of them is difficult to be handled in the model. For example, the thermal transfer resistance in SiB2, Noah, and CLM is lower than the observed one for arid and semi-arid conditions [*Yang et al*., 2009b], which further changes surface energy partition [*Chen et al*., 2010, 2011; *Liu et al*., 2012]. However, its effect on the simulation of soil moisture is indirect and needs further investigations. Furthermore, the uncertainties in available soil texture and other parameter databases should not be ignored. The simulation error sources are indentified at an alpine grassland site with Noah model. We found that the soil texture-induced error is minor than the SOC-induced error (not shown).

5. Conclusions

[28] In this study, we evaluated four AMSR-E soil moisture products and four GLDAS soil moisture outputs against the ground measurement at two spatial scales ($1^\circ \times 1^\circ$and $0.25^\circ \times 0.25^\circ$) in the central Tibetan Plateau, which is a cold semi-arid region with low biomass.

[29] Compared to the ground truth, the four AMSR-E products have large discrepancies in this region. In terms of the mission requirement of $RMSE < 0.06\,m^3\,m^{-3}$, none of them provides reliable estimates in the unfrozen season (May to October). The JAXA, LPRM_C, and LPRM_X products can reflect the soil moisture dynamic range but give too large seasonal amplitude, whereas the NASA product exhibits a dampened range of soil moisture. The JAXA product gives the smallest *BIAS*, while the NASA product evidently underestimates the soil moisture and LPRM products have large positive biases. These suggest that AMSR-E soil moisture retrieval algorithms need more improvements in cold semi-arid regions.

[30] The GLDAS LSMs systematically underestimate the moisture within the topsoil but well simulate the soil moisture below the topsoil. Compared with AMSR-E algorithms, the GLDAS LSMs give low *RMSE* and *BIAS* values except the Mosaic model. However, the errors in GLDAS are still large, and the R^2 of GLDAS products are lower than those of the satellite products. The cause for the systematic underestimation in the simulations is due to the absence of high amount of soil organic carbon, which was found in the central TP.

[31] The evaluation in this study assumes that the arithmetic average over station-measured soil moisture represents the ground truth. In consideration of high spatial variability of soil moisture, the assumption may lead to uncertainties in the evaluation. To reduce this uncertainty, it is indispensable to up-scale soil moisture from point measurements to areal average.

[32] **Acknowledgments.** This work was jointly supported by CMA Special Fund for Scientific Research in the Public Interest (Grant No. GYHY201206008), National Natural Science Foundation of China (Grant Nos. 41105003 and 41171268), and Open Fund from the State Key Laboratory of Remote Sensing Science (Grant No. OFSLRSS201108) that is cosponsored by the Institute of Remote Sensing Applications of Chinese Academy of Sciences and Beijing Normal University.

References

Albergel, C., P. de Rosnay, C. Gruhier, J. Muñoz-Sabater, S. Hasenauer, L. Isaksen, Y. Kerr, and W. Wagner (2012), Evaluation of remotely sensed and modelled soil moisture products using global ground-based in situ observations, *Remote Sens. Environ.*, *118* (15), 215–226, doi:10.1016/j.rse.2011.11.017.

Balsamo, G., A. Beljaars, K. Scipal, P. Viterbo, B. van den Hurk, M. Hirschi, and A. Betts (2009), A revised hydrology for the ECMWF model: Verification from field site to terrestrial water storage and impact in the Integrated Forecast System, *J. Hydrometeor.*, *10*, 623–643, doi:10.1175/2008JHM1068.1.

Bitar, A., D. Leroux, Y. Kerr, O. Merlin, P. Richaume, A. Sahoo, and E. Wood (2012), Evaluation of SMOS soil moisture products over continental U.S. using the SCAN/SNOTEL network, *IEEE Trans. Geosci. Remote Sens.*, *50*(5), 1572–1586, doi:10.1109/TGRS.2012.2186581.

Boisserie, M., D. Shin, T. LaRow, and S. Cocke (2006), Evaluation of soil moisture in the Florida State University climate model–National Center for Atmospheric Research community land model (FSU-CLM) using two reanalyses (R2 and ERA40) and in situ observations, *J. Geophys. Res.*, *111*, D08103, doi:10.1029/2005JD006446.

Brocca, L., et al. (2011), Soil moisture estimation through ASCAT and AMSR-E sensors: An intercomparison and validation study across Europe, *Remote Sens. Environ.*, *115*, 3390–3408, doi:10.1016/j.rse.2011.08.003.

Chen, Y., K. Yang, W. Tang, J. Qin, and L. Zhao (2012), Parameterizing soil organic carbon's impacts on soil porosity and thermal parameters for Eastern Tibet grasslands, *Sci. China Ser. D.*, *55*(6), 1001–1011, doi:10.1007/s11430-012-4433-0.

Chen, Y., K. Yang, J. He, J. Qin, J. Shi, J. Du, and Q. He (2011), Improving land surface temperature modeling for dry land of China, *J. Geophys. Res.*, *116*, D20104, doi:10.1029/2011JD015921.

Chen, Y., K. Yang, D. G. Zhou, J. Qin, X. F. Guo (2010), Improving the Noah land surface model in arid regions with an appropriate parameterization of the thermal roughness length, *J. Hydrometeor.*, *11*, 995–1006. doi: 10.1175/2010JHM1185.1.

Collow, T., A. Robock, J. Basara, and B. Illston (2012), Evaluation of SMOS retrievals of soil moisture over the central United States with currently available in situ observations, *J. Geophys. Res.*, *117*, D09113, doi:10.1029/2011JD017095.

Crow, W., A. Berg, M. Cosh, A. Loew, B. Mohanty, R. Panciera, P. de Rosnay, D. Ryu, and J. Walker (2012), Upscaling sparse ground-based soil moisture observations for the validation of coarse-resolution satellite soil moisture products, *Rev. Geophys.*, *50*, RG2002, doi:10.1029/2011RG000372.

Dall'Amico, J., F. Schlenz, A. Loew, and W. Mauser (2012), First results of SMOS soil moisture validation in the upper Danube catchment, *IEEE Trans. Geosci. Remote Sens.*, *50*(5), 1507–1516, doi:10.1109/TGRS.2011.2171496.

de Jeu, R., W. Wagner, T. Holmes, A. Dolman, N. van de Giesen, and J. Friesen (2008), Global soil moisture patterns observed by space borne microwave radiometers and scatterometers, *Surv. Geophys.*, *29*(4), 399–420, doi:10.1007/s10712-008-9044-0.

Dorigo, W., K. Scipal, R. Parinussa, Y. Liu, W. Wagner, R. de Jeu, and V. Naeimi (2010), Error characterisation of global active and passive microwave soil moisture datasets, *Hydrol. Earth Syst. Sci.*, *14*, 2605–2616, doi:10.5194/hess-14-2605-2010.

Dorigo, W. et al. (2011), The International Soil Moisture Network: A data hosting facility for global in situ soil moisture measurements, *Hydrol. Earth Syst. Sci.*, *15*(5), 1675–1698. doi:10.5194/hessd-8-1609-2011.

Douville, H., and F. Chauvin (2000), Relevance of soil moisture for seasonal climate predictions: A preliminary study, *Clim. Dynam.*, *16*, 719–736, doi:10.1007/s003820000080.

Draper, C., J. Walker, P. Steinle, R. de Jeu, and T. Holmes (2009), An evaluation of AMSR-E derived soil moisture over Australia, *Remote Sens. Environ.*, *113*, 703–710, doi:10.1016/j.rse.2008.11.011.

Entekhabi, D. et al. (2010), The Soil Moisture Active and Passive (SMAP) Mission, *Proceedings of the IEEE*, 98(5).

Falloon, P., C. Jones, M. Ades, and K. Paul (2011), Direct soil moisture controls of future global soil carbon changes: An important source of uncertainty, *Global Biogeochem. Cycles*, *25*, GB3010, doi:10.1029/2010GB003938.

Fujii, H., T. Koike, and K. Imaoka (2009), Improvement of AMSR-E Algorithm for soil moisture estimation by introducing a fractional vegetation coverage dataset derived from MODIS data, *J. Remote Sens. Soc. Jpn.*, *29*(1), 282–292.

Gherboudj, I., R. Magagi, K. Goïta, A. Berg, B. Toth, and A. Walker (2012), Validation of SMOS data over agricultural and boreal forest areas in Canada, *IEEE Trans. Geosci. Remote Sens.*, *50*(5), 1623–1635, doi:10.1109/TGRS.2012.2188532.

Gruhier, C. et al. (2010), Soil moisture active and passive microwave products: Intercomparison and evaluation over a Sahelian site, *Hydrol. Earth Syst. Sci.*, *14*(1), 141–156, doi:10.5194/hess-14-141-2010.

Jackson, T. J. (1993), III. Measuring surface soil moisture using passive microwave remote sensing, *Hydrol. Process.*, *7*(2), 139–152, doi: 10.1002/hyp.3360070205.

Jackson, T., M. Cosh, R. Bindlish, P. Starks, D. Bosch, M. Seyfried, D. Goodrich, S. Moran, and J. Du (2010), Validation of advanced microwave scanning radiometer soil moisture products, *IEEE Trans. Geosci. Remote Sens.*, *48*(12), 4256–4272, doi:10.1109/TGRS.2010.2051035.

Jackson, T., R. Bindlish, M. Cosh, T. Zhao, P. Starks, D. Bosch, M. Seyfried, M. Moran, D. Goodrich, Y. Kerr, D. Leroux (2012), Validation of Soil Moisture and Ocean Salinity (SMOS) soil moisture over watershed networks in the U.S., *IEEE Trans. Geosci. Remote Sens.*, *50* (5), 1530–1543. doi:10.1109/TGRS.2011.2168533.

Kerr, Y. et al. (2012), The SMOS soil moisture retrieval algorithm, *IEEE Trans. Geosci. Remote Sens.*, *50*(5), 1384–1403. doi:10.1109/TGRS.2012.2184548.

Koike, T., Y. Nakamura, I. Kaihotsu, G. Davva, N. Matsuura, K. Tamagawa, and H. Fujii (2004), Development of an Advanced Microwave Scanning Radiometer (AMSR-E) algorithm of soil moisture and vegetation water content, *Annu. J. Hydraul. Eng., Jpn. Soc. Civil Eng.*, *48*(2), 217–222.

Koster, R., P. Dirmeyer, et al. (2004), Regions of strong coupling between soil moisture and precipitation, *Science*, *305*(5687), 1138–1140, doi:10.1126/science.1100217.

Lacava, T., P. Matgen, L. Brocca, M. Bittelli, N. Pergola, T. Moramarco, and V. Tramutoli (2012), A first assessment of the SMOS soil moisture product with in situ and modeled data in Italy and Luxembourg, *IEEE Trans. Geosci. Remote Sens.*, *50*(5), 1612–1622, doi:10.1109/TGRS.2012.2186819.

Lawrence, D., A. Slater (2008), Incorporating organic soil into a global climate model, *Clim. Dyn.*, *30*, 145–160, doi:10.1007/s00382-007-0278-1.

Li, H., A. Robock, and M. Wild (2007), Evaluation of Intergovernmental Panel on Climate Change fourth assessment soil moisture simulations for the second half of the twentieth century, *J. Geophys. Res.*, *112*, D06106, doi:10.1029/2006JD007455.

Liu, Y., Q. He, H. Zhang, and A. Mamtimin (2012), Improving the CoLM in Taklimakan Desert hinterland with accurate key parameters and an appropriate parameterization scheme, *Adv. Atmos. Sci.*, *29*(2), 381–390, doi: 10.1007/s00376-011-1068-6.

Lu, H., T. Koike, H. Fujii, T. Ohta, and K. Tamagawa (2009), Development of a physically-based soil moisture retrieval algorithm for spaceborne passive microwave radiometers and its application to AMSR-E, *J. Remote Sens. Soc. Jpn.*, *29*(1), 253–262.

Merlin, O., C. Rüdiger, A. Bitar, P. Richaume, J. Walker, and Y. Kerr (2012), Disaggregation of SMOS soil moisture in Southeastern Australia, *IEEE Trans. Geosci. Remote Sens.*, *50*(5), 1556–1571, doi:10.1109/TGRS.2011.2175000.

Milly, P., and K. Dunne (1994), Sensitivity of the global water cycle to the water-holding capacity of land, *J. Climate*, *7*, 506–526.

Njoku, E., and S. Chan (2006), Vegetation and surface roughness effects on AMSR-E land observations, *Remote Sens. Environ.*, *100*, 190–199, doi:10.1016/j.rse.2005.10.017.

Njoku, E., T. Jackson, V. Lakshmi, T. Chan, and S. Nghiem (2003), Soil moisture retrieval from AMSR-E, *IEEE Trans. Geosci. Remote Sens.*, *41*, 215–229, doi:10.1109/TGRS.2002.808243.

Owe, M., R. de Jeu, and T. Holmes (2008), Multisensor historical climatology of satellite-derived global land surface moisture, *J. Geophys. Res.*, *113*, F01002, doi:10.1029/2007JF000769.

Paloscia, S., G. Macelloni, and E. Santi (2006), Soil moisture estimates from AMSR-E brightness temperatures by using a dual-frequency algorithm, *IEEE Trans. Geosci. Remote Sens.*, *44*, 3135–3144.

Prigent, C., F. Aires, W. Rossow, and A. Robock (2005), Sensitivity of satellite microwave and infrared observations to soil moisture at a global scale: Relationship of satellite observations to in situ soil moisture measurements, *J. Geophys. Res.*, *110*, D07110, doi:10.1029/2004JD005087.

Qin, J., K. Yang, S. Liang, X. Guo (2009), The altitudinal dependence of recent rapid warming over the Tibetan Plateau, *Clim. Chang.*, *97*(1), 321–327, doi:10.1007/s10584-009-9733-9.

Rodell, M. et al. (2004), The global land data assimilation system, *Bull. Amer. Meteor. Soc.*, *85*(3), 381–394.

Rüdiger, C., J. Calvet, C. Gruhier, T. Holmes, R. de Jeu, and W. Wagner (2009), An intercomparison of ERS-Scat and AMSR-E soil moisture observations with model simulations over France, *J. Hydrometeor*, *10*, 431–447. doi:10.1175/2008JHM997.1

Sánchez, N., J. Martínez-Fernández, A. Scaini, and C. Pérez-Gutiérrez (2012), Validation of the SMOS L2 soil moisture data in the REMEDHUS network (Spain), *IEEE Trans. Geosci. Remote Sens.*, *50* (5), 1602–1611, doi:10.1109/TGRS.2012.2186971.

Schaap, M. G., L. de Lange, T. J. Heimovaara (1996), TDR calibration of organic forest floor media, *Soil Technol.*, *11*, 205–217.

Schmugge, T. (1977), Remote sensing of surface soil moisture, *J. Appl. Meteorol.*, *17*, 1549–1557.

Scipal, K., T. Holmes, R. de Jeu, V. Naeimi, and W. Wagner (2008), A possible solution for the problem of estimating the error structure of global soil moisture data sets, *Geophys. Res. Lett.*, *35*, L24403, doi:10.1029/2008GL035599.

Scipal, K., Z. Bartalis, S. Hasenauer, and W. Wagner (2009), An improved soil moisture retrieval algorithm for ERS and METOP scatterometer observations, *IEEE Trans. Geosci. Remote Sens.*, *47*(7), 1999–2013, doi:10.1109/TGRS.2008.2011617.

Su, Z., J. Wen, L. Dente, R. van der Velde, L. Wang, Y. Ma, K. Yang, Z. Hu (2011), The Tibetan Plateau observatory of plateau scale soil moisture and soil temperature (Tibet-Obs) for quantifying uncertainties in coarse resolution satellite and model products, *Hydrol. Earth Syst. Sci.*, *15*(7), 2303–2316, doi:10.5194/hess-15-2303-2011.

Wagner, W., K. Scipal, C. Pathe, D. Gerten, W. Lucht, and B. Rudolf (2003), Evaluation of the agreement between the first global remotely sensed soil moisture data with model and precipitation data, *J. Geophys. Res.*, *108*(D19), 4611, doi:10.1029/2003JD003663.

Yang, K., B. Ye, D. Zhou, B. Wu, T. Foken, J. Qin, and Z. Zhou (2011), Response of hydrological cycle to recent climate changes in the Tibetan Plateau, *Clim. Chang.*, *109*(3), 517–534, doi:10.1007/s10584-011-0099-4.

Yang, K., J. He, W. Tang, J. Qin, C. C. K. Cheng (2010), On downward shortwave and longwave radiations over high altitude regions: Observation and modeling in the Tibetan Plateau, *Agr. Forest Meteorol.*, *150*, 38–46, doi:10.1016/j.agrformet.2009.08.00.

Yang, K., T. Koike, I. Kaihotsu, and J. Qin (2009a), Validation of a dual-pass microwave land data assimilation system for estimating surface soil moisture in semi-arid regions, *J. Hydrometeorol.*, *10*(3), 780–794, doi: 10.1175/2008JHM1065.1.

Yang K., Y. Chen, and J. Qin (2009b), Some practical notes on the land surface modeling in the Tibetan Plateau, *Hydrol. Earth Syst. Sci.*, *13*, 687–701, doi:10.5194/hess-13-687-2009.

Yang, K., T. Koike, B. Ye, and L. Bastidas (2005), Inverse analysis of the role of soil vertical heterogeneity in controlling surface soil state and energy partition, *J. Geophys. Res.*, *110*, D08101, doi:10.1029/2004JD005500.